Recombinant dimeric PDZ protein inhibitors for long-term relief of chronic pain by AAV therapeutics

Gith Noes-Holt[a], Kathrine L. Jensen[a], Mette Richner[b], Raquel C. Baro[a], Line Sivertsen[a], Sara E. Jager[a], Lucía J. Fernández[a], Rita C. Andersen[a], Jamila H. Lilja[a], Andreas H. Larsen[a], Nikolaj R. Christensen[a], Anke Tappe-Theodor[c], Christian B. Vægter[b], Rohini Kuner[c], Kenneth L. Madsen[a], Andreas T. Sørensen[a,1]

a. Molecular Neuropharmacology and Genetics Laboratory, Department of Neuroscience, Faculty of Health and Medical Sciences, University of Copenhagen, Denmark

b. Dandrite, Department of Biomedicine, Aarhus University, Denmark

c. Institute of Pharmacology, Heidelberg University, Heidelberg, Germany

1. To whom correspondence should be addressed: andreass@sund.ku.dk

Abstract

Chronic pain is estimated to affect 20% of the adult population, and the burden on individual patients and society caused by chronic pain is escalating. Current treatments, including opioids, anti-convulsants, and anti-depressants, are only moderately effective and limited by severe side effects and addiction liability. The inadequate state of current treatment, the chronic nature of particularly neuropathic pain, and the high impact on quality of life render chronic pain conditions relevant for gene therapy. Here, we describe the development of a self-assembling, bivalent peptide inhibitor of the pain-associated scaffold protein PICK1, delivered by adeno-associated viral (AAV) vectors. This strategy prevents mechanical allodynia in mouse inflammatory and neuropathic pain models and reverses neuropathic pain in advanced stages for an entire year. Pain relief was obtained by selective targeting of several relays along the somatosensory pain pathways without observed side effects. Importantly, full pain relief was also achieved by selective transduction of peripheral neurons, which is highly attractive for therapeutic intervention since it is less likely to cause intolerable side effects.

Introduction

Exploiting gene therapies for refractory pain conditions holds promise to overcome several adversities of current pain medicine, including low efficacy, dose-limiting side effects, and opioid addiction [1,2]. Today's drawbacks not only inflict on clinical practice and patient quality of life but also come with severe socioeconomic consequences, which the present opioid epidemic unquestionably confirms[3]. It is estimated that one out of five adults in the US is affected by chronic pain[4], of which approximately half suffer from chronic neuropathic pain[5]. This condition arises from a lesion or disease of the somatosensory nervous system[6], and no single treatment to cure or prevent neuropathic pain is currently available.

The most used gene therapy vector for nervous system application, and considered the safest, is the adeno-associated viral (AAV) vector. It is characterized by its replication-deficient, low immunogenic, and long-lasting expression profile without the need for repeated dosing[2,7]. Its innate ability to deliver therapeutic gene expression locally and within a defined cell population, not hindered by membrane barriers, adds powerful dimensions to how AAVs can be tailored for disease treatment. While current treatments for neuropathic pain exclusively target receptors and transporters[8], we envision that targeting intracellular pathways underlying the development of chronic pain conditions might be more efficacious and circumvent systemic side effects.

Synaptic PDZ (PSD-95/DLG-1/ZO-1) domain scaffold proteins regulate discrete and dynamic functions of signaling events, such as protein transport, ion channel signaling, and other signal systems through protein-protein interactions[9,10]. As such, they are vital for the integrity and modulation of neuronal communication and therefore putative clinically relevant pain targets. Several synthetic peptide inhibitors that can block specific PDZ domain interactions have been developed to modulate synaptic efficacy[11-15]. Characterized by their C-terminal residues, typical 5-13 amino acids of length and with the identical motif of a known interacting partner protein, these peptides are designed to interrupt specific protein-protein interactions. Notably, peptides that target PSD-95 and disrupts the NMDA-type ionotropic glutamate receptor-dependent signaling can attenuate animal pain-related behaviors[16,17]. We recently addressed another PDZ scaffold protein, PICK1 (Protein Interacting with C-Kinase 1), as a potent target for pain[14,18]. This protein is highly conserved, expressed in neuronal tissue across species, and best known for its trafficking role in regulating AMPA-type ionotropic glutamate receptor surface expression at synapses[19-21]. We constructed a synthetic bivalent peptide targeting PICK1 having two C-terminal HWLKV-motifs fused by a PEG-linker and conjugated to the Tat-sequence, rendering it cell-permeable[14]. Intrathecal (i.t.) administration of this PICK1

targeting peptide fully reversed mechanical allodynia for hours in the spared-nerve injury (SNI) model of neuropathic pain. Surprisingly, efficacy was only evident for a bivalent and not an analogous, monovalent peptide inhibitor[14].

In the current study, we conceived an AAV-based strategy that allows recombinant peptide inhibitors to posttranslationally assemble into a dimeric configuration thereby positioning two C-terminal HWLKV-motifs freely exposed to interact with PICK1. We assessed the therapeutic efficacy of this approach in mouse pain models and harnessed the ability of AAV for effective and selective expression of the peptide within neurons. We further combined this strategy with LoxP recombination approaches and capsid technology to determine the site of action. Our data revealed that various pain modalities in both inflammatory and neuropathic pain models were completely prevented or reversed with a duration of up to one year after treatment and without causing side effects. Targeting either the PNS or CNS, we observed that both interventions were sufficient to completely reverse pain hypersensitivity, which all together supports PICK1 as a compelling target for unmanageable pain conditions qualified for AAV gene therapy.

Results

High-affinity recombinant bivalent peptides targeting PICK1 prevent inflammation-induced mechanical allodynia. Inspired by our previous work on a synthetic bivalent peptide inhibitor of PICK1, TPD5[14,18], we conceived a molecular design enabling posttranslational self-assembly of a monomeric peptide, encoded by the AAV vector, into a dimer. This gene cassette, consisting of an N-terminal dimerization domain originating from yeast basic-region leucine zipper (bZIP) transcription factor (GCN4), a flexible glycine linker region (GGGGS), and a C-terminal PICK1 PDZ-binding motif (HWLKV), was created in two basic configurations. One variant with the native aspartic acid (D) and serine (S) in position 7 and 14, respectively, and another variant with two prolines (P) at the same positions within GCN4 (**Figure 1A**) predicted to render the homo-dimerization more dynamic (**Suppl. Figure 1A-C**). Biochemical experiments confirmed that the self-assembly of the peptides indeed demonstrated PICK1 binding avidity (GCN4-HWLKV, $K_{i,App}$ = 119 nM; GCN4(7P14P), $K_{i,App}$ = 548 nM) (**Suppl. Figure 2A**) and that GCN4-HWLKV, but not GCN4(7P14P)-HWLKV, drove PICK1 oligomerization (**Suppl. Figure 2B-E**), similar to the bivalent peptide, TPD5[14]. To obtain selective and constitutive pan-neuronal expression, the peptide gene cassette was driven by the human synapsin (hSyn) promoter. AAV vectors were manufactured in-house, including the two putative therapeutic vectors: AAV-Di-C5 (AAV8-hSyn-GCN4-HWLKV) and AAV-Di(7P14P)-C5 (AAV8-hSyn-GCN4(7P14P)-HWLKV). Cortical neuronal cultures were transduced with either these vectors or two

negative control vectors, AAV-tdTomato (AAV8-hSyn-tdTomato) and AAV-Di-GS (AAV8-hSyn-GCN4-GGGGS-GGGGS) and processed for GCN4 immunocytochemistry for validation of transgene peptide expression (**Figure 1B**). Peptide expression was confined to the cytoplasm and excluded from the nucleus. We next tested the vectors in the Complete Freund's Adjuvant (CFA) model of inflammatory pain, where the level of mechanical allodynia, determined as the paw withdrawal threshold to stimulation by von Frey filaments, was measured repeatedly before and after a single i.t. injection at L5-L6 lumbar level in wild-type (WT) male mice. Both the AAV-Di-C5 and AAV-Di(7P14P)-C5 vectors prevented the development of allodynia, whereas AAV-tdTomato injected mice developed significant allodynia as expected in the days following intraplantar CFA injection (**Figure 1C**). The pain threshold remained unaltered in the non-inflamed (contralateral) paw, regardless of treatments (**Figure 1C**), suggesting an analgesic effect of the two active recombinant peptides without numbing (anesthetizing) mechanical sensitivity. After 11 days, the paw withdrawal threshold for AAV-tdTomato returned to previous baseline levels, highlighting the transient nature of this model. Subsequently, the opioid receptor antagonist naltrexone (NTX) was administered once on day 11 and again on day 40 to reinstate allodynia[22]. In this situation, AAV-Di-C5 and AAV-Di(7P14P)-C5, but not AAV-tdTomato, prevented mechanical allodynia demonstrating an extended duration of action (**Figure 1C**). The chronic nature of the AAV intervention renders it difficult to discern whether the treatment simply relieves the NTX-induced hyperalgesia or rather prevents the underlying plasticity of the opioid system so that NTX no longer reinstates hyperalgesia. Other AAVs, with modified gene cassettes encoding EGFP fusion or EGFP-P2A self-cleavage linked peptides, were also efficacious in this CFA experiment (**Suppl. Figure 3A**). Next, we tested the effect of AAV-Di-C5 and AAV-tdTomato on heat-induced hyperalgesia. CFA injection induced a significant reduction in threshold temperature in AAV-tdTomato injected animals, whereas this reduction was smaller and non-significant for AAV-Di-C5 injected mice. However, the threshold temperature for AAV-Di-C5 mice was not significantly different from AAV-tdTomato mice (**Suppl. Figure 3B**), suggesting a partial relief of heat hyperalgesia in addition to the full relief of mechanical allodynia.

To probe target engagement and specificity, we performed pull-down experiments using synthetic biotinylated GCN4-peptides, either containing the HWLKV motif designed for targeting PICK1 or the IETDV motif previously used for targeting PSD-95[13]. Western blots of peptide-spiked tissue lysates from the brain stem, spinal cord, and dorsal root ganglions (DRGs) demonstrated robust target engagement and clear selectivity towards PICK1 and PSD-95, respectively (**Figure 1D-E**). Finally, we asked whether the pain-relieving effects of the high-affinity PICK1 inhibitors were dependent on the GCN4 dimerization domain or the PDZ-binding sequence, HWLKV. First, we exchanged GCN4 with alternative dimerization domains; AAV-

Atg16-C5, AAV-Mdv1-C5, and AAV-SSO10a-C5 having either longer lengths or antiparallel orientations (**Figure 1F-G**). AAV-Atg16-C5 and AAV-Mdv1-C5 were too long for synthetic production, but biochemical experiments with the AAV-SSO10a-C5 peptide confirmed that antiparallel self-assembly mediated by SSO10a helix conferred avidity for PICK1 binding and drove PICK1 tetramerization similar to GCN4 (**Suppl. Figure 4A-E**). Secondly, we substituted the PDZ-binding sequence, HWLKV, with a second copy of the linker sequence, GGGGS, to yield GCN4-GS. Biochemical experiments validated the intact helical and dimeric assembly, while PICK1 binding and tetramerization were abolished (**Suppl. Figure 4A-D, F**). Upon i.t. administration of AAV-GCN4-GS, mice developed mechanical hyperalgesia in the CFA model similar to the negative control, AAV-tdTomato (**Figure 1C**). In contrast, injection of AAV-Di-C5 again significantly alleviated mechanical allodynia, demonstrating the critical role of the PDZ-binding motif (**Figure 1F-G**). Next, injection of AAV-Atg16-C5, AAV-Mdv1-C5, or AAV-SSO10a-C5 relieved mechanical allodynia to varying extents, with AAV-Atg16-C5 not being significantly different from AAV-GCN4-GS (**Figure 1F-G**). This demonstrates that the observed treatment effects were not dependent on the GCN4 motif itself. In contrast, the varying effect of the substitution for GCN4 might reflect differences in dimerization strength, steric hindrance, expression level, etc. To this end, we concluded that different high-affinity recombinant bivalent peptides, targeting PICK1 and delivered by AAV, are able to prevent mechanical allodynia in the CFA mouse model, even during NTX-induced hyperalgesia reinstatement suggesting a non-opioid analgesic profile on nociceptive pain. We decided, therefore, to further characterize the expression and efficacy profiles of AAV-Di-C5 and AAV-Di(7P14P)-C5 vectors.

Targeting neurons below the cervical spinal level can reverse mechanical allodynia. To determine which neurons contributed to the pain-relieving effect following i.t. AAV administration, we took advantage of the transgenic mouse line, Hoxb8-Cre. This mouse expresses Cre recombinase under the control of the *Hoxb8* gene and is confined to neurons caudally to the cervical level 3-7 of the spinal cord, including the DRGs[23]. Cre-dependent AAVs were designed to achieve confined peptide expression by exploiting a Cre-ON (AAV8-DIO[EGFP-P2A-Di-C5]ON) and Cre-OFF (AAV8-DIO[EGFP-P2A-Di-C5]OFF) approach (**Figure 2A and Suppl. Figure 5A-B**). We again used the CFA model to first confirm the robustness of the AAVs in WT mice. In WT-mice, the OFF-variant, designed to express the Di-C5 peptide constitutively in non-Cre expressing neurons, fully prevented the development of mechanical allodynia (**Figure 2B-C**) in agreement with our previous result (**Figure 1C**). As expected, the ON-variant was in contrast without effect in WT animals (**Figure 2B-C**). However, when tested on Hoxb8-Cre mice of mixed genders and within the same experiment as for their WT littermates, the Cre-ON variant fully abolished mechanical allodynia. The Cre-OFF variant, on the other

hand, displayed a trending, but non-significant treatment effect (**Figure 2B-C**), reflecting that transgene expression selectively below the cervical level 3-7 is sufficient to prevent mechanical allodynia.

To obtain insight into the transduction profile following i.t. delivery of the recombinant AAV, we next used the Cre-reporter mouse line, Ai14, that expresses robust tdTomato fluorescence following Cre-mediated recombination (**Suppl. Figure 6A)**. For this purpose, we employed an AAV similar to AAV-Di-C5 (**Suppl. Figure 3A),** but now additionally encoding iCre fused to EGFP (AAV8-iCre:EGFP-P2A-Di-C5). Mice examined 44 days following i.t. injection of AAV exhibited clear tdTomato signals within neuronal cell bodies of DRGs at sacral and lumbar segments (**Figure 2D**) with clearly visible ascending fibers confined within the spinal cord dorsal column (**Figure 2E, Suppl. Figure 6B**) consistent with robust transduction of mechanosensitive Aβ fibers. This labeling pattern was accompanied by thin fibers extending into the spinal cord dorsal horn laminae (**Figure 2E**), but it is unclear whether these fibers are of nociceptive origin. The tdTomato fluorescence along the spinal cord terminated at the dorsal column nuclei in the closed medulla oblongata (cuneate and gracile nuclei) and did not extend further rostrally from the pons. However, sparse labeling of individual neuronal cell bodies was observed in the brain, e.g., in the cerebellum and olfactory structures (**Figure 2F, Suppl. Figure 6B**). Little if any expression was observed in cell bodies within the spinal cord at the lumbar level (**Figure 2E**). This expression pattern suggests that AAV8, after i.t. injection, predominantly transduces DRGs having fibers extending into local spinal circuits but with very noticeable projections extending to supraspinal sites. The Ai14 mice of mixed gender also did not develop mechanical allodynia in the CFA model, suggesting that these tdTomato-expressing neurons are sufficient for pain relief by AAV-Di-C5 (**Suppl. Figure 6C)**. Further examination revealed that transduced tdTomato-positive DRG neurons, which were immunoreactive for IB4, CGRP, or NF200 markers, only comprised a fraction of all DRGs (**Figure 2G, H**), and were significantly shifted towards larger DRG neurons (**Figure 2H**). While smaller DRG neurons consisted mainly of IB4+ or CGRP+ neurons, the larger DRG neurons were mainly comprised by CGRP+ or NF200+ neurons (**Figure 2I**). In a separate cohort of WT mice, we saw that mRNA levels of the peptide were high in DRGs of AAV-Di-C5 as compared to vehicle (DPBS) injected mice (**Figure 2J, Suppl. Table 1**), in accordance with the observation made from Ai14 mice. In the adjacent sciatic nerve and lumbar spinal cord tissue, mRNA peptide levels were also detectable, but not equally prominent. In all other tissue examined, except for the liver, peptide mRNA was not identified (**Figure 2J, Suppl. Table 1)**.

Complete prevention and reversal of chronic neuropathic pain by AAV-encoded PICK1 inhibitors.
Neuropathic pain often develops into a chronic condition which is very challenging to treat efficiently. Hence, we next assessed the efficacy of the AAVs in the spared-nerve injury (SNI) mouse model of

neuropathic pain. In a preventative treatment paradigm, where the AAVs were i.t. injected 14 days before SNI surgery in WT mice, mechanical allodynia was again determined by paw withdrawal threshold using von Frey filaments. Following the SNI procedure, AAV-tdTomato, as well as vehicle (DPBS), treated mice showed robust and comparable levels of mechanical allodynia up to 28 days after SNI, whereas AAV-Di-C5 and AAV(7P14P)-C5 completely prevented allodynia as compared to AAV-tdTomato and vehicle (**Figure 3A**). These findings prompted us to further assess the treatment efficacy and robustness in the SNI model. When AAV was delivered five weeks following SNI injury, at a stage when the initial inflammation is ceased, mechanical allodynia from week 9 after SNI and until the end of the experiment at week 25 was significantly attenuated when comparing AAV-Di(7P14P)-C5 and AAV-tdTomato treated mice (**Figure 3B**). Next, we assessed the long-term efficacy of the intervention, where SNI mice were repeatedly monitored for an entire year. With i.t. injections performed on day 2 after injury, AAV-Di(7P14P)-C5 significantly reversed mechanical allodynia for 52 weeks, except at week 46, as compared to AAV-tdTomato (**Figure 3C**). Based on these findings, we concluded that the recombinant peptides can prevent the development and reverse an already established mechanical allodynia in both acute and chronic stages of neuropathic pain and maintain efficacy for at least 1 year in mice.

The AAV-encoded PICK1 inhibitor reduces several sensory pain modalities induced by SNI. Neuropathic pain conditions typically manifest within several pain modalities. Therefore, we tested WT mice receiving AAV-Di(7P14P)-C5 or AAV-tdTomato across other pain modalities associated with SNI, now including both SNI and sham groups. Similar to the 1-year experiment, i.t. injections were performed on day 2 after injury (**Suppl. Figure 7A**). We first confirmed by von Frey stimulations that mechanical allodynia was successfully established before the AAV intervention in this cohort, and in line with previous results (**Figure 3C**), injection of AAV-Di(7P14P)-C5 completely attenuated mechanical allodynia in SNI mice (**Suppl. Figure 7B**). Sham mice did not show any change in paw withdrawal threshold (**Suppl. Figure 7B**). In the dynamic mechanical allodynia test, using dynamic (brush) instead of static (von Frey hairs) touch, averaged response scores were increased after SNI (compared to sham) and were significantly lower following expression of AAV-Di(7P14P)-C5 as compared to AAV-tdTomato at day 40, whereas responses in both sham groups were unchanged (**Figure 3D**). For cold allodynia tested on a 2°C cold plate, mice subjected to SNI displayed a much lower response latency on day 6 following injury. SNI mice treated with AAV-Di(7P14P)-C5 showed a significant recovery in their response latency on day 35 and not on day 41 compared to mice injected with AAV-tdTomato, albeit with considerable variations, which was not observed for the other groups (**Figure 3E**). Similarly, the application of acetone to probe cold allodynia caused aggravated nocifensive behaviors in both SNI groups, but with trending, yet non-significant, treatment effects seen for SNI mice treated with

AAV-Di(7P14P)-C5 (compared to AAV-tdTomato) (**Figure 3F**). As an index of spontaneous pain, we finally quantified the number of spontaneous paw lifts (SPL)[24] for 15 min on day 46 and day 70. While sham mice, regardless of treatments, had almost no SPL, this behavior was prominent in the SNI groups but significantly reduced in mice receiving AAV-Di(7P14P)-C5 (compared to AAV-tdTomato) (**Figure 3G**). This suggested that not only provoked but also ongoing spontaneous pain behaviors were attenuated by the treatment. Further, along with this battery of testing, all mice across groups were temporally exposed to automatic monitoring in single-cages for determining potential changes in voluntary behaviors, including rearing, grooming, climbing, immobility, and locomotion. No differences were found between any of the groups (**Figure 3H, Suppl. Figure 7C-I**). Summarized, this series of behavioral assays support that several sensory pain modalities caused by chronic nerve injury, including dynamic and static tactile allodynia, as well as spontaneous pain behavior, can be attenuated by AAV encoding recombinant peptides targeting PICK1 whereas thermal allodynia is less well treated.

AAV-encoded PICK1 inhibitor neither improve motor deficits nor alter normal motor functions. Next, we asked whether the therapeutic intervention could reverse any motor function deficits associated with SNI. Again, we monitored the same SNI and sham groups of mice receiving either AAV-tdTomato or AAV-Di(7P14P)-C5. In CatWalk, SNI mice had significantly lower max contact area and swing speed of the injured paw than sham mice, but no treatment changes were seen across groups (**Suppl. Figure 8A-B**). On the contrary, average run speed and duration in CatWalk were unaffected by SNI and again not affected by treatments across groups (**Suppl. Figure 8C-D**). In voluntary wheel running, sham mice ran significantly longer than SNI mice, but no treatment difference was observed within treatment groups (**Suppl. Figure 8E)**. This data supports that gross motor deficits caused by peripheral nerve transection cannot be attenuated by recombinant PICK1 inhibitors. Apart from this, body weight was monitored periodically over 91 days, with no clear changes seen over time across treatments (**Suppl. Figure 8F**). Other phenotypical changes (nest building, social behavior, muscle weakness, etc.) were also not noticed by the experimenters throughout. In summary, these data support that general well-being and health status remain unperturbed by the treatments but with some evident SNI-induced motor deficiencies.

We next i.t. injected naïve mice with AAV-Di-C5, AAV-tdTomato, or vehicle (DPBS) to further assess potential side effects of the AAVs (**Figure 4A**). In a 2-hour open field test completed 35 days following i.t. injection, total distance traveled, and time spent in center and border zones did not differ between treatment groups (**Figure 4B-D, Suppl. Figure 9A**). Mice were also subjected to RotaRod. Latency to fall and best speed obtained using accelerating speed remained unaffected across groups (**Figure 4E**). Likewise, in

the RotaRod fixed speed test, no significant difference was found between treatment groups when comparing latency to fall and the best speed obtained (**Figure 4F**). Together this suggests that the AAVs cause no major impact on motor coordination in uninjured mice. We finally verified the efficacy of the AAVs in this setup by subjecting the mice to CFA. Levels of mechanical allodynia indeed confirmed that AAV-Di-C5, but not by AAV-tdTomato and vehicle treatment, fully alleviated inflammation-induced mechanical allodynia (**Suppl. Figure 9B**), in accordance with previous results (**Figure 1D**). Together, these results argue that AAV-encoded recombinant peptides targeting PICK1 selectively affects maladaptive pain signaling circuits and processing without alternating gross motor or proprioceptive control in healthy intact circuits.

Systemic AAV delivery selectively targeting either CNS or PNS, completely alleviates neuropathic pain. Novel AAV capsids, like the PHP.s and PHP.eb, can selectively transduce either CNS or PNS, respectively[25]. Motivated by our previous observations that targeting DRGs seems to play a primary role in suppressing pain by the recombinant peptides delivered by AAV serotype 8, we wanted to test if exclusive peripheral expression would be equally efficacious. AAVs encoding recombinant peptides were packaged into PHP.s or PHP.eb capsids. Mechanical allodynia, repeatedly measured by von Frey stimulation, was confirmed before WT mice were intravenously (i.v.) into mice on day 37 after SNI surgery. Control groups receiving either vehicle (DPBS) or AAVPHP.s-iCre:EGFP displayed mechanical allodynia after SNI and did not recover, while mice receiving the PNS (AAVPHP.s-iCre:EGFP-P2A-Di-C5, or PHP.s) or CNS (AAVPHP.eb-iCre:EGFP-P2A-Di-C5, or PHP.eb) targeting capsids recovered completely, as measured 125 days after SNI and 88 days after i.v. injection (**Figure 5A**). Transduction profiles of the AAVs were examined in Ai14 mice receiving identical dosing. The AAVPHP.s capsid gave rise to clear tdTomato labeling of DRG neuronal cell bodies and dorsal column fibers in the spinal cord and brainstem (**Figure 5B**), almost identical to i.t injected mice exposed to AAV8 vector (**Figure 2D-F, Suppl. Figure 6B**). Importantly, few tdTomato-positive neurons were observed within CNS without region specificity (**Figure 5B**). In contrast, the PHP.eb capsid gave rise to strong tdTomato expression in neurons of the spinal cord, brainstem, and brain, while DRG neurons were not labeled (**Figure 5C**). This pattern was corroborated by the EGFP signal confined towards cell bodies in spinal cord and distributed across the brain (**Figure 5C**). In summary, the data supports that systemic delivery of recombinant peptides targeting either PNS or CNS can fully attenuate chronic neuropathic pain. However, we cannot rule out whether the scanty CNS neurons transduced by PHP.s could be involved, although this seems unlikely. Interestingly, long-term expression of recombinant peptides did not induce any observable side-effect, even following extensive CNS exposure provided by PHP.eb. This further supports PICK1 as a

compelling pain target and highlights that therapeutic interventions directed towards PICK1 may not only be envisioned as a treatment for chronic neuropathic pain originating from PNS but also CNS.

Discussion

Very few treatments for neuropathic pain show long-lasting benefits. Despite the obvious unmet medical need, developing an analgesic with better efficacy and fewer side effects has failed. AAV-based gene therapy is a new therapeutic frontier in medicine and offers the potential to address significant unmet clinical needs, including the treatment of pain conditions.

In this study, we developed a novel AAV gene therapy, where the pain-relieving effects were confirmed across three different academic institutions. We show that our intervention can prevent and reverse chronic neuropathic pain across different sensory modalities by AAV-encoded recombinant bivalent peptides designed to target PICK1 with high affinity. PICK1 is an interesting scaffold protein in the context of pain. It plays a central role in synaptic plasticity and interacts with several partners of relevance to pain, including several glutamate receptors (GRIK1, GRIK2, GRIK4, GRK7), in addition to the AMPA receptor subunit (GRIA2 and 3), acid-sensing ion channels (ASIC1 and 2), aquaporin (AQP1) and protein kinase C-alpha (PKA-C)[26]. Furthermore, PICK1 is highly conserved and expressed within neurons of both rodents and humans along the somatosensory nociceptive pathway, including DRGs, substantiating that PICK1 is indeed a relevant therapeutic pain target[26]. This is also supported by studies in animal models using inhibitory peptides, siRNA, and knock-out mice, where the lack of PICK1 function was shown to decrease hyperexcitable pain conditions[27-30]. PICK1 is known as a gatekeeper that controls the balance between calcium-impermeable and CP-AMPARs[31-33]. Along these lines, a peripherally applied CP-AMPAR antagonist can alleviate chronic pain without affecting mechanosensation or eliciting central side effect[34] in concordance with current data. That said, we still do not know the significance of other potential PICK1 partners that may also contribute to the effect, also because of limited insight into PICK1 function in DRGs.

The i.t. and i.v. delivery routes using AAV8 and PHP.s, respectively, in Ai14 mice showed that the recombinant peptides predominantly transduced DRG neurons and were more or less absent from neurons of the spinal cord and supraspinal regions. This was further supported by the mRNA peptide profile obtained from WT mice. In accordance, i.t. injection of AAV8-GFP in rats resulted in labeling of the dorsal column fibers and DRG neurons at all levels, but with no neuronal cell bodies found outside the DRGs[35]. This indicates that the therapeutic effect, as seen in these settings, involves ascending dorsal column medial lemniscus (DCML) fibers. This pathway, consisting of Aβ low-threshold mechanoreceptor (LTMR) fibers, normally transmits non-noxious mechanosensory information, whereas nociceptive signaling is

mediated by the small unmyelinated C fibers or thinly myelinated Aδ fibers. However, nerve injury may cause a phenotypic switch in which Aβ fibers acquire nociceptive capacity[36]. Notably, tactile allodynia induced by spinal nerve L5/L6 ligation in rats was abolished following complete dorsal column lesion without causing motor deficits[37], and optogenetics activation of non-nociceptive Aβ fibers following peripheral nerve injury drove tactile allodynia[38]. Needless to say, if this peripheral mechanism of action is equally efficacious in humans, the side-effect profile envisioned will be very different from existing therapeutics for the treatment of neuropathic pain and very likely more benevolent.

When packaged with the PHP.eb capsid, transduction and expression of the AAV were restricted exclusively towards neurons in the CNS covering the entire spinal cord and supraspinal areas. Here, equally potent treatment efficacy on mechanical allodynia was seen, suggesting that the recombinant peptides, including PICK1 as a target in pain, may even be of clinical relevance for central neuropathic pain conditions. The long-lasting efficacy for at least 1 year further argues that the mechanism of action is not prone to desensitization. Given that clinical AAV gene therapy is extraordinarily expensive and neutralizing antibodies strongly limit AAV vectors for repeated administration, long duration is also key for this type of intervention. Taken together, the present work provides evidence that AAV-encoded bivalent peptide inhibitors designed to target PICK1 can effectively provide long-term relief of chronic pain and may represent a promising therapeutic option that can be viewed as a one-shot, lifetime treatment.

Methods and materials

All information is provided as Supplementary Information.

Author contributions

GNH cloned all plasmids, produced all AAV vectors, performed most experiments, completed histology, and did all data analysis. KLJ, MR and CBV were involved in SNI experiments. KLJ was involved in SNI and CFA experiments. LJF was involved in CFA experiments and tissue processing. RCB assisted with AAV production, tissue processing, and staining. LS assisted with tissue processing and pull-down experiments. SEJ assisted with tissue processing and performed the immunohistochemistry. RCA and JHL performed qPCR experiments. AHL conducted MD simulations. NRC performed parts of the biochemistry analysis. ATT, CBV, RK, KLM, and ATS supervised the research. GNH, KLM, and ATS conceptualized the study, designed the research, and interpreted data. NRC, KLM, and ATS invented the recombinant dimeric peptides. GNH and

ATS wrote the manuscript with contributions from KLM. All authors reviewed and critically evaluated the manuscript.

Competing interest statement

The recombinant dimeric peptides, their usage, and their extended utilization are disclosed in two patent applications currently being processed at the European Patent office (EPO) and the United States Patent and Trademark Office (USPTO). KLM and ATS have ownership interest and are co-founders of Zyneyro, a company having exclusive license rights on the two patents, which are owned by the University of Copenhagen, Denmark. All other authors have no competing interest to declare.

Acknowledgment

We thank Lone Rosenquist and Nabeela Khadim for excellent technical assistance, and Prof. Ole Kiehn for generous access to transgenic animals. We acknowledge the Core Facility for Integrated Microscopy, Faculty of Health and Medical Sciences, University of Copenhagen. This work was supported by a Novo Nordisk Foundation Pre-seed grant (KLM, ATS), Lundbeck Foundation grant R344-2020-1063 (KLM), Independent Research Fund Denmark 2025-00028B (GNH), Innovation Fund Denmark grant 9122-00012B (ATS), the Augustinus Foundation grant 17-3517 (ATS) and the A.P. Møller Foundation grants 18-L-0213 (ATS) and L-2021-0031(ATS).

Legends to main figures

Figure 1. AAV-encoded dimeric peptides designed for targeting PICK1 fully abolish CFA-induced mechanical allodynia.

A) From conceptual design to the expression of two bivalent peptide inhibitors with HWLKV motifs for targeting PICK1, but with different amino acid compositions at positions 7 and 14 within the GCN4 helical structure.

B) ICC performed on cortical neuronal cultures transduced with different AAV variants, showing GCN4 immunoreactivity (green), DAPI nuclei staining (blue) and tdTomato autofluorescence (red) (for AAV-tdTomato only).

C) Tactile sensitivity measured by von Frey before and after i.t. injection of AAVs, and again after CFA and NTX administration, as indicated. Paw withdrawal threshold of AAV-tdTomato (control; ipsilateral paw) was

compared to AV-Di-C5 and AAV-Di(7P14P)-C5 treatment conditions, including the two EGFP containing vectors shown in Suppl. Figure 3A. $^{**}P < 0.01$, $^{***}P < 0.001$, $^{****}P < 0.0001$. Two-way repeated measures ANOVA, $F(32, 208) = 2.198$; Dunnett's multiple comparison; N = 6-8 per group.

D) Western blot of PICK1 following pull-down from the brain stem, spinal cord, and brain tissue homogenate spiked with biotinylated peptides. Bio-GCN4-HWLKV and Bio-GCN4(7P14P)-HWLKV peptides are designed to target PICK1, whereas Bio-GCN4-GS is a negative control, and Bio-GCN4-IETDV has a binding motif for targeting PSD-95.

E) Western blot of PSD-95 in a similar setup as in panel D.

F) Test of different AAV-encoded peptides in the CFA model measuring paw withdrawal threshold before and after i.t. injection and after CFA administration, where AAV-Di-C5, AAV-SSO10a-C5, AAV-Mdv1-C5, AAV-Atg16-C5, and AAV-Di-GS (non-binding variant) treatments were compared. $^{*}P < 0.05$, $^{**}P < 0.01$, $^{****}P < 0.0001$. Two-way repeated measures ANOVA, $F(12, 57) = 2.449$; Tukey's multiple comparison; N = 4-6 per group.

G) Illustration of AAV-encoded recombinant peptides variants, including the non-binding GCN4-GS variant and the three PICK1-binding variants (SSO10a, Atg16, Mdv1) having alternative dimerization domains of different lengths and orientations.

Abbreviations: BL, baseline; i.t., intrathecal; NTX, naltrexone. All data are shown as mean with s.e.m.

Figure 2. Dimeric peptide delivery towards DRGs and spinal cord fully abolish CFA-induced mechanical allodynia.

A) Layout showing peptide expression in Hoxb8-Cre and WT mice using an ON-OFF viral targeting approach. With this, peptide expression can be restricted exclusively to neurons expressing Cre-recombinase or not, as indicated.

B) Tactile sensitivity determined by paw withdrawal threshold before and after i.t. injection of AAVs and after intraplantar CFA administration in Hoxb8-Cre and WT mice using the ON-OFF strategy. $^{**}P < 0.01$, $^{****}P < 0.0001$. Two-way repeated measures ANOVA, $F(9, 93) = 3.800$; Tukey's multiple comparisons; N = 7-10 per group. Abbreviations: BL = baseline.

C) Day 4 from experiment in panel B. Data in B and C is shown as mean with s.e.m.

D) AAV8-iCre:EGFP-P2A-Di-C5 vector i.t injected into Ai14 reporter mice for determining bivalent peptide expression, showing tdTomato-labeled neurons within lumbar (L1-L5) and sacral (S1-S2) DRGs.

E) Coronal section of the spinal cord at the lumbar level with notable tdTomato labeled projections within the dorsal column spinal cord comprising ascending fibers from DRG neurons (Insert I). Within the grey matter of the dorsal horn, fibers, but not neurons, were visible (insert II, gain adjusted).

F) Sagittal brain section with tdTomato-positive fibers within the brain stem (Insert III) terminating within cuneate and gracile nuclei (Insert IV) and not extending rostrally into periaqueductal gray (PAG) and beyond. The bottom three panels are gain adjusted. Abbreviations: AP = area postrema, AQ = cerebral aqueduct, ECU = external cuneate nucleus, CU = cuneate nucleus, cuf = cuneate fascicle, GR = gracile nucleus.

G) Representative images of neuronal cell bodies in the DRG show immunostaining with markers IB4, CGRP, and NF200 (top panels) with tdTomato as a marker for viral transduction (middle panels) and merged images (bottom panels). Arrows mark double positive neurons.

H) Histogram displaying numbers and cross-sectional area of neuronal cell bodies from L3 and L4 DRG. All neurons = 1367, tdTomato-positive neurons = 224. *N* = 3 mice. Insert: Cumulative distribution of all neurons and tdTomato-positive neurons as a function of their cross-sectional area. ****$P < 0.0001$; Kolmogorov-Smirnov test.

I) The relative distribution of all neurons (solid grey area/line) plotted together with the relative distribution of all transduced neurons (solid red area) as a function of their cross-sectional area. The dotted lines show the cross-sectional area of neurons positive for IB4, CGRP and NFAP markers, respectively. *N* = 40-44 neurons per marker.

J) Peptide mRNA expression levels in DRGs from L3-L5 (both sides), sciatic nerve, lumbar spinal cord, and pons evaluated by RT-qPCR. Mice received i.t. injection of either AAV8-GCN4-Di-C5 or vehicle (DPBS). ***$P < 0.001$. Unpaired t-test, t(4) = 10.87. *N* = 4 per group. Data is shown as mean with s.e.m.

Figure 3. AAV-encoded dimeric peptide targeting PICK1 revokes SNI-induced allodynia for at least one year.

A) Paw withdrawal threshold in WT mice before and after i.t. injection and after SNI in a preventative treatment paradigm, where AAVs or vehicle (DPBS) are administered before SNI surgery. **$P < 0.01$, ***$P < 0.001$, ****$P < 0.0001$. Two-way repeated measures ANOVA, F(18, 126) = 5.474; Tukey's multiple comparisons; *N* = 5-8 per group.

B) Paw withdrawal threshold in WT mice before and after SNI surgery, with i.t. AAV injection performed 5 weeks post SNI surgery. *$P < 0.05$, **$P < 0.01$, ***$P < 0.001$, ****$P < 0.0001$. Two-way repeated measures ANOVA, F(9, 93) = 5.474; Holm-Šidák's multiple comparisons; *N* = 7-8 per group.

C) One-year treatment assessment. Paw withdrawal threshold in WT mice before and after SNI surgery, and with i.t. AAV injection performed 2 days after SNI surgery. *$P < 0.05$, ***$P < 0.001$, ****$P < 0.0001$. Two-way repeated measures ANOVA, F(20, 360) = 8.305; Holm-Šidák's multiple comparisons; *N* = 10 per group.

D) Paw withdrawal reaction score following brushing of the hind paw before and after SNI or sham surgery with i.t. AAV injection performed 2 days post SNI or sham surgery. ***$P < 0.001$, Two-way repeated measures ANOVA, F(6, 38) = 9.971, Tukey's multiple comparisons; $N = 6$ per group.

E) Latency for first paw withdrawal on a 2°C cold plate before and after SNI or sham surgery with i.t. AAV injection performed 2 days post SNI or sham surgery. **$P < 0.01$. Two-way repeated measures ANOVA, F(9, 57) = 13.39, Tukey's multiple comparisons; $N = 6$ per group.

F) Total time exhibiting nocifensive behavior for 60 seconds following a drop of acetone applied to the ipsilateral paw before and after SNI or sham surgery with i.t. AAV injection performed 2 days post SNI or sham surgery. **$P < 0.01$. One-way repeated measures ANOVA, F(3, 19) = 9.101, Tukey's multiple comparisons; $N = 5$-6 per group.

G) Number of spontaneous paw lifts (ipsilateral) recorded over 15 min in SNI or sham surgery mice after i.t. AAV injection. *$P < 0.05$, ***$P < 0.001$, ****$P < 0.0001$. Two-way repeated measures ANOVA, F(3, 19) = 5.013, Tukey's multiple comparisons; $N = 5$-6 per group.

H) Automatic cage monitoring of general behavior during 22 hours in sham or SNI animals following i.t. injection of AAVs using the Laboras system. Percentages of time spent for each classified behavior are shown. Individual scores and statistics are provided in Suppl. Figure 7C-I.

Abbreviations: BL = baseline, i.t. = intrathecal. All data in A-G are shown as mean with s.e.m.

Figure 4. Unperturbed motor function performance following AAV dimeric peptide treatment.

A) Study layout and timeline.

B) Total distance traveled in a 2-hour open field test for naïve animals receiving either i.t. injection of AAVs or vehicle (DPBS). One-way ANOVA, F(2, 13) = 0.979; Tukey's multiple comparisons. $N = 5$-6 per group

C) Time spent in the center zone in the same test as panel B. One-way ANOVA, F(2, 13) = 0.583; Tukey's multiple comparisons.

D) Time spent in the border zone in the same setup as panel B. One-way ANOVA, F(2, 13) = 0.584; Tukey's multiple comparisons.

E) Same mice as in panel B were examined on the accelerating RotaRod for time to fall (left) and best speed obtained (right). Time to fall: One-way ANOVA, F(2, 13) = 0.671; Tukey's multiple comparisons. Best speed: One-way ANOVA, F(2, 13) = 0.620; Tukey's multiple comparisons. Average scores of 3 trials per mouse.

F) Same mice as in panel B were examined in the fixed-speed RotaRod paradigm. Fall is shown as a survival probability. AAV-Di-C5 vs. AAV-tdTomato: Log-rank (Mantel-Cox) test, Chi-square = 0.089; AAV-Di-C5 vs.

vehicle: Log-rank (Mantel-Cox) test, Chi-square = 0.916. Panel insert: Best speed obtained. One-way ANOVA, F(2, 13) = 0.648; Tukey's multiple comparisons.

Abbreviations: i.t. = intrathecal; OFT, Open Field Test. All data in B-F are shown as mean with s.e.m.

Figure 5. Systemic AAV delivery of dimeric PICK1 inhibitor targeting either CNS or PNS fully alleviates SNI-induced mechanical allodynia.

A) Paw withdrawal threshold in Ai14 mice before and after SNI surgery and after systemic AAV administration (intravenous, i.v., injection) of AAVs with PHP.eb, PHP.s capsids or vehicle (DPBS). *$P < 0.05$, **$P < 0.01$. Two-way repeated measures ANOVA, F(5, 100) = 3.727; Dunnett's multiple comparisons (AAV-PHP.s-iCre:EGFP serving as control); $N = 6$ per group. Abbreviations: i.v. = intravenous. Data are shown as mean with s.e.m.

B) TdTomato signaling from Ai14 mice in panel A receiving AAV-PHP.s-iCre:EGFP-P2A-Di-C5 vector with fluorescent fibers along the spinal cord dorsal column at all levels and with labeled cell somas within the DRGs. Ascending fibers terminate at the cuneate and gracile nuclei within the brain stem. Expression of EGFP is visible in DRGs only.

C) Same as for panel B, but for Ai14 mice receiving AAV-PHP.eb-iCre:EGFP-P2A-Di-C5 vector. tdTomato signaling is excluded from DRGs, but notable throughout the spinal cord and brain. EGFP expression is confined to cell bodies in the spinal cord (green dots) and distributed across the brain.

Legends to Supplementary Figures

Supplementary Figure 1. Self-assembly and helicity are more pronounced for Bio-GCN4-HWLKV than for Bio-GCN4(7P14P)-HWLKV peptides.

A) Molecular dynamics simulation for estimation of the free energy of dimerization, which were 84.4 ± 3.7 kJ/mol for Bio-GCN4-HWLKV (purple) and 60.9 ± 3.4 kJ/mol for Bio-GCN4(7P14P)-HWLKV (lavender). The free energy was shown as mean with s.e.m. from $N = 5$ simulation per peptide.

B) Fast-protein liquid chromatography (FPLC) trace of Bio-GCN4-HWLKV (purple) and Bio-GCN4(7P14P)-HWLKV (lavender) peptides (10 µM) for assessment of their oligomeric state.

C) Circular dichroism spectra of Bio-GCN4-HWLKV (purple) and Bio-GCN4(7P14P)-HWLKV (lavender) peptides (30 µM) for assessment of their secondary structure.

Supplementary Figure 2. PICK1 binding and oligomerization are more pronounced for Bio-GCN4-HWLKV than for Bio-GCN4(7P14P)-HWLKV peptides

A) Fluorescence competition binding curves for Bio-GCN4-HWLKV (purple), Bio-GCN4(7P14P)-HWLKV (lavender), and HWLKV (gray) peptides using a constant concentration of PICK1 and 5FAM-DATC5 (20 nM) as a tracer. Apparent Ki values from the binding curves are shown to the right, *N* = 6.

B-E) Fast-protein liquid chromatography (FPLC) traces of PICK1 **B)** alone (cyan) (40 µM), **C)** with Bio-GCN4-HWLKV (lavender) (molar ratio 1:4), **D)** Bio-GCN4(7P14P)-HWLKV (purple) (molar ratio 1:4) and **E)** with Bio-GCN4-HWLKV (lavender) (molar ratio 1:2). Gray columns indicate elution volume of the peptides alone from Suppl. Figure 1B.

Supplementary Figure 3. AAVs with EGFP fusion cassettes are equally efficacious in the CFA model.

A) Tactile sensitivity measured by von Frey stimulation before and after i.t. injection of AAVs, and again after CFA and NTX administration as indicated. Paw withdrawal threshold (ipsilateral) comparison was made between AAV-tdTomato (control) and the two EGFP-containing vectors, including AAV-Di-C5 and AAV-Di(7P14P)-C5 from Figure 1, as testing of these vectors was completed within the same experiment. $*P < 0.05$, $**P < 0.01$, $***P < 0.001$, $****P < 0.0001$. Two-way repeated measures ANOVA, $F(32, 208) = 2.198$; Dunnett's multiple comparisons; *N* = 5-8 per group. Abbreviations: BL = baseline, i.t. = intrathecal, NTX = naltrexone.

B) Temperature for the first nocifensive response on the dynamic hot plate in CFA and naïve mice, i.t. injected with AAV-tdTomato or AAV-Di-C5. $*P < 0.05$, $**P < 0.01$. One-way ANOVA, $F(3, 36) = 4.971$; Tukey's multiple comparisons; *N* = 8-10 per group.

All data in A-B are shown as mean with s.e.m.

Supplementary Figure 4. Substitution of the PDZ binding sequence abolishes PICK1 binding and oligomerization, whereas substitution of the dimerization motifs is tolerated.

A) Fluorescence competition binding curves for Bio-GCN4-HWLKV (lavender), Bio-SSO10a-HWLKV (orange), Bio-GCN4-GGGGS (gray), and HWLKV (black) peptides using a constant concentration of PICK1 and 5FAM-DATC5 (20 nM) as tracer. Relative affinities are shown to the right, n = 3.

B) Fast-protein liquid chromatography (FPLC) traces of Bio-GCN4-HWLKV (lavender), Bio-SSO10a-HWLKV (orange), and Bio-GCN4-GGGGS (gray) (20 µM) for assessment of their oligomeric state.

C) Circular dichroism spectra of Bio-SSO10a-HWLKV (orange) and Bio-GCN4-GGGGS (gray) peptides (30 µM) for assessment of their secondary structure.

D-F) Fast-protein liquid chromatography (FPLC) traces of **D)** PICK1 (cyan) (40 µM) with Bio-GCN4-HWLKV (lavender) (molar ratio 1:2), **E)** PICK1 (cyan) (40 µM) with Bio-SSO10a-HWLKV (orange) (molar ratio 1:2) and **F)** PICK1 (cyan) (40 µM) with Bio-GCN4-GGGGS (gray) (molar ratio 1:2).

Supplementary Figure 5. ON/OFF AAV-targeting strategy in Hoxb8-Cre mice.

A) With the ON/OFF AAV targeting strategy, transgene expression will either be restricted to Hoxb8-Cre or non-Cre expressing cells. For the OFF-strategy, expression is limited rostrally from cervical levels 3-7 of the spinal cord (brain stem, brain), whereas, for the ON-strategy, expression is limited to the spinal cord and DRGs.

B) Construct validation in WT mice. The OFF-strategy gives rise to constitutive expression of the transgene (EGFP:iCre and the recombinant peptide), whereas for the ON-strategy, the transgene will not be expressed.

Supplementary Figure 6. Robust AAV transduction of DCML fibers following intrathecal AAV8 injection into Ai14 mice.

A) Ai14 transgenic mice harboring a lox-stop-lox (LSL)-tdTomato cassette controlled by the CAG promoter in the Rosa26 locus (Rosa-CAG-LSL-tdTomato) were i.t. injected with AAV-hSyn-iCre:EGFP-P2A-Di-C5. The cre-dependent tdTomato fluorescent signal allows for precise identification of neurons and circuits transduced by the injected AAV vector.

B) Following i.t. AAV injection in Ai14 mice, tdTomato-positive fibers are visible within the spinal cord dorsal column at the sacral, lumbar, thoracic, and cervical levels. These fibers originate from DRG neurons. The AAV has limited access to the brain, with sparse tdTomato-positive neurons (tdTomato-positive) were found across different brain regions. This sagittal brain slice is an example showing limited transduction of neurons within the cerebellum and olfactory system. The sparse labeling of the brain was consistent but varied across brain regions in different animals. All scalebars represents 500 µm.

C) Paw withdrawal threshold measured before and after intraplantar CFA administration in Ai14 reporter mice i.t. injected with AAV8-iCre:EGFP-P2A-Di-C5. Two-way repeated measures ANOVA, $F(2, 12) = 3.146$; Tukey's multiple comparisons; $N = 4$ per group, mixed genders. Abbreviations: BL = baseline.

Supplementary Figure 7. Confirmation of treatment in SNI animals and cage monitoring of general behavior using the Laboras system.

A) Study layout and timeline.

B) Mechanical allodynia (paw withdrawal threshold) in WT mice before and after SNI or sham surgery with i.t. AAV injection with AAV-Di(7P14P)-C5 or AAV-tdTomato performed 2 days post SNI and sham surgery. ****$P < 0.0001$; Two-way ANOVA, F(6, 38) = 9.390; Tukey's multiple comparisons; N = 5-6 per group. Abbreviations: BL = baseline, i.t. = intrathecal.

C-I) General behaviors were monitored for 22 hours on days 55-58 after SNI or sham surgery using individual Laboras-specific cages and monitoring system. All comparisons were one-way ANOVA with Tukey's multiple comparisons and were all non-significant. N = 5-6 per group.

Data in B-I are shown as mean with s.e.m.

Supplementary Figure 8. Influence of AAV treatment on locomotion and weight following SNI surgery.

A) Max contact area of the ipsilateral paw determined by CatWalk in WT mice before and after SNI or sham surgery with i.t. AAV injections of AAV-Di(7P14P)-C5 or AAV-tdTomato performed 2 days post SNI or sham surgery. Mean of three trials at each time point. Two-way repeated measures ANOVA, F(9, 57) = 6.855; Tukey's multiple comparisons; N = 5-6 per group.

B) As in panel A, but for the swing speed of the ipsilateral paw. Mean of three trials at each time point. Two-way repeated measures ANOVA, F(9, 57) = 2.140; Tukey's multiple comparisons; N = 5-6 per group.

C) As in panel A, but for average speed. Mean of three trials at each time point. Two-way repeated measures ANOVA, F(9, 57) = 0.9906; Tukey's multiple comparisons; N = 5-6 per group.

D) As in panel A, but for the run duration. Mean of three trails at each time point. Two-way repeated measures ANOVA, F(9, 57) = 0.7267; Tukey's multiple comparisons; N = 5-6 per group.

E) Average distance of voluntary wheel running during the night-time (18:00-06:00) as measured 3 times in the same animals (SNI and sham-operated mice with AAV-Di(7P14P)-C5 or AAV-tdTomato). *$P < 0.05$, **$P < 0.01$, ***$P < 0.001$; One-way ANOVA, F(9, 19) = 10.32; Tukey's multiple comparison; N = 5-6 per group.

F) Body weight measured on multiple occasions from the day of SNI surgery in SNI and sham-operated mice with AAV-Di(7P14P)-C5 or AAV-tdTomato. **$P < 0.01$ (comparing sham w. AAV-Di(7P14P vs. SNI w. AAV-tdTomato from day 33-91). Two-way repeated measures ANOVA, F(30, 190) = 2.703; Tukey's multiple comparisons; N = 5-6 per group.

Abbreviations: BL = baseline, ipsi = ipsilateral. All data in A-F are shown as mean with s.e.m.

Supplementary Figure 9. Time course of open field test and validation of AAV treatments.

A) Two hours open field test showing distance traveled (5 min binned) for AAV-Di-C5, AAV-tdTomato and vehicle-treated mice. Two-way repeated measures ANOVA, $F(46, 299) = 1.097$; Dunnett's multiple comparisons; N = 5-6 per group.

B) Validation of the treatments in the CFA model following the behavioral assays. ***$P < 0.001$, ****$P < 0.0001$; Two-way ANOVA, $F(2, 13) = 7.428$; Tukey's multiple comparisons; N = 5-6 per group. Abbreviations: i.t. = intrathecal.

All data in A-B are shown as mean with s.e.m.

Supplementary Table 1. Quantitative real-time PCR (qRT-PCR) of mRNA transcription of peptide and housekeeping genes in various tissues.

Mean Ct values with standard deviation (from 4 animals, each with 3 technical replicates) are shown for each primer target and tissue type. Mean Ct values are subsequently normalized to the expression of housekeeping genes (Methods, qPCR, equation 1) (values not shown). The relative change in peptide expression compared to the control group, DPBS, are expressed as mean ΔΔCt values with standard deviation for each treatment group (Methods, qPCR, equation 2). P-values are shown (unpaired t-test) when comparing the relative expression (expressed as ΔΔCt) in the treatment group, AAV-Di-C5, to the control group, DPBS.

References

1 Deverman, B. E., Ravina, B. M., Bankiewicz, K. S., Paul, S. M. & Sah, D. W. Y. Gene therapy for neurological disorders: progress and prospects. *Nat Rev Drug Discov* **17**, 641-659, doi:10.1038/nrd.2018.110 (2018).

2 Kuzmin, D. A. *et al.* The clinical landscape for AAV gene therapies. *Nat Rev Drug Discov* **20**, 173-174, doi:10.1038/d41573-021-00017-7 (2021).

3 Hedegaard, H., Minino, A. M. & Warner, M. Drug Overdose Deaths in the United States, 1999-2019. *NCHS Data Brief*, 1-8 (2020).

4 Dahlhamer, J. *et al.* Prevalence of Chronic Pain and High-Impact Chronic Pain Among Adults - United States, 2016. *MMWR Morb Mortal Wkly Rep* **67**, 1001-1006, doi:10.15585/mmwr.mm6736a2 (2018).

5 van Hecke, O., Austin, S. K., Khan, R. A., Smith, B. H. & Torrance, N. Neuropathic pain in the general population: a systematic review of epidemiological studies. *Pain* **155**, 654-662, doi:10.1016/j.pain.2013.11.013 (2014).

6 Finnerup, N. B., Kuner, R. & Jensen, T. S. Neuropathic Pain: From Mechanisms to Treatment. *Physiol Rev* **101**, 259-301, doi:10.1152/physrev.00045.2019 (2021).

7 Hudry, E. & Vandenberghe, L. H. Therapeutic AAV Gene Transfer to the Nervous System: A Clinical Reality. *Neuron* **102**, 263, doi:10.1016/j.neuron.2019.03.020 (2019).
8 Fornasari, D. Pharmacotherapy for Neuropathic Pain: A Review. *Pain Ther* **6**, 25-33, doi:10.1007/s40122-017-0091-4 (2017).
9 Feng, W. & Zhang, M. Organization and dynamics of PDZ-domain-related supramodules in the postsynaptic density. *Nat Rev Neurosci* **10**, 87-99, doi:10.1038/nrn2540 (2009).
10 Kim, E. & Sheng, M. PDZ domain proteins of synapses. *Nat Rev Neurosci* **5**, 771-781, doi:10.1038/nrn1517 (2004).
11 Aarts, M. *et al.* Treatment of ischemic brain damage by perturbing NMDA receptor- PSD-95 protein interactions. *Science* **298**, 846-850, doi:10.1126/science.1072873 (2002).
12 Brebner, K. *et al.* Nucleus accumbens long-term depression and the expression of behavioral sensitization. *Science* **310**, 1340-1343, doi:10.1126/science.1116894 (2005).
13 Bach, A. *et al.* A high-affinity, dimeric inhibitor of PSD-95 bivalently interacts with PDZ1-2 and protects against ischemic brain damage. *Proc Natl Acad Sci U S A* **109**, 3317-3322, doi:10.1073/pnas.1113761109 (2012).
14 Christensen, N. R. *et al.* A high-affinity, bivalent PDZ domain inhibitor complexes PICK1 to alleviate neuropathic pain. *EMBO Mol Med* **12**, e11248, doi:10.15252/emmm.201911248 (2020).
15 Li, P. *et al.* AMPA receptor-PDZ interactions in facilitation of spinal sensory synapses. *Nat Neurosci* **2**, 972-977, doi:10.1038/14771 (1999).
16 D'Mello, R., Marchand, F., Pezet, S., McMahon, S. B. & Dickenson, A. H. Perturbing PSD-95 interactions with NR2B-subtype receptors attenuates spinal nociceptive plasticity and neuropathic pain. *Mol Ther* **19**, 1780-1792, doi:10.1038/mt.2011.42 (2011).
17 Tao, F., Su, Q. & Johns, R. A. Cell-permeable peptide Tat-PSD-95 PDZ2 inhibits chronic inflammatory pain behaviors in mice. *Mol Ther* **16**, 1776-1782, doi:10.1038/mt.2008.192 (2008).
18 Jensen, K. L., Noes-Holt, G., Sorensen, A. T. & Madsen, K. L. A Novel Peripheral Action of PICK1 Inhibition in Inflammatory Pain. *Front Cell Neurosci* **15**, 750902, doi:10.3389/fncel.2021.750902 (2021).
19 Hanley, J. G. PICK1: a multi-talented modulator of AMPA receptor trafficking. *Pharmacol Ther* **118**, 152-160, doi:10.1016/j.pharmthera.2008.02.002 (2008).
20 Clem, R. L., Anggono, V. & Huganir, R. L. PICK1 regulates incorporation of calcium-permeable AMPA receptors during cortical synaptic strengthening. *J Neurosci* **30**, 6360-6366, doi:10.1523/JNEUROSCI.6276-09.2010 (2010).
21 Gardner, S. M. *et al.* Calcium-permeable AMPA receptor plasticity is mediated by subunit-specific interactions with PICK1 and NSF. *Neuron* **45**, 903-915, doi:10.1016/j.neuron.2005.02.026 (2005).
22 Corder, G. *et al.* Constitutive mu-opioid receptor activity leads to long-term endogenous analgesia and dependence. *Science* **341**, 1394-1399, doi:10.1126/science.1239403 (2013).
23 Witschi, R. *et al.* Hoxb8-Cre mice: A tool for brain-sparing conditional gene deletion. *Genesis* **48**, 596-602, doi:10.1002/dvg.20656 (2010).
24 Lee, K. S., Huang, Y. H. & Yen, C. T. Periaqueductal gray stimulation suppresses spontaneous pain behavior in rats. *Neurosci Lett* **514**, 42-45, doi:10.1016/j.neulet.2012.02.053 (2012).
25 Chan, K. Y. *et al.* Engineered AAVs for efficient noninvasive gene delivery to the central and peripheral nervous systems. *Nat Neurosci* **20**, 1172-1179, doi:10.1038/nn.4593 (2017).
26 Sorensen, A. T., Rombach, J., Gether, U. & Madsen, K. L. The Scaffold Protein PICK1 as a Target in Chronic Pain. *Cells* **11**, doi:10.3390/cells11081255 (2022).
27 Atianjoh, F. E. *et al.* Spinal cord protein interacting with C kinase 1 is required for the maintenance of complete Freund's adjuvant-induced inflammatory pain but not for incision-induced post-operative pain. *Pain* **151**, 226-234, doi:10.1016/j.pain.2010.07.017 (2010).
28 Garry, E. M. *et al.* Specific involvement in neuropathic pain of AMPA receptors and adapter proteins for the GluR2 subunit. *Mol Cell Neurosci* **24**, 10-22, doi:10.1016/s1044-7431(03)00134-9 (2003).

29 Wang, W. *et al.* Preserved acute pain and impaired neuropathic pain in mice lacking protein interacting with C Kinase 1. *Mol Pain* **7**, 11, doi:10.1186/1744-8069-7-11 (2011).
30 Wang, Z. *et al.* PICK1 Regulates the Expression and Trafficking of AMPA Receptors in Remifentanil-Induced Hyperalgesia. *Anesth Analg* **123**, 771-781, doi:10.1213/ANE.0000000000001442 (2016).
31 Famous, K. R. *et al.* Phosphorylation-dependent trafficking of GluR2-containing AMPA receptors in the nucleus accumbens plays a critical role in the reinstatement of cocaine seeking. *J Neurosci* **28**, 11061-11070, doi:10.1523/JNEUROSCI.1221-08.2008 (2008).
32 Bellone, C. & Luscher, C. Cocaine triggered AMPA receptor redistribution is reversed in vivo by mGluR-dependent long-term depression. *Nat Neurosci* **9**, 636-641, doi:10.1038/nn1682 (2006).
33 Anggono, V., Clem, R. L. & Huganir, R. L. PICK1 loss of function occludes homeostatic synaptic scaling. *J Neurosci* **31**, 2188-2196, doi:10.1523/JNEUROSCI.5633-10.2011 (2011).
34 Gangadharan, V. *et al.* Peripheral calcium-permeable AMPA receptors regulate chronic inflammatory pain in mice. *J Clin Invest* **121**, 1608-1623, doi:10.1172/JCI44911 (2011).
35 Jacques, S. J. *et al.* AAV8(gfp) preferentially targets large diameter dorsal root ganglion neurones after both intra-dorsal root ganglion and intrathecal injection. *Mol Cell Neurosci* **49**, 464-474, doi:10.1016/j.mcn.2012.03.002 (2012).
36 Neumann, S., Doubell, T. P., Leslie, T. & Woolf, C. J. Inflammatory pain hypersensitivity mediated by phenotypic switch in myelinated primary sensory neurons. *Nature* **384**, 360-364, doi:10.1038/384360a0 (1996).
37 Sun, H. *et al.* Nerve injury-induced tactile allodynia is mediated via ascending spinal dorsal column projections. *Pain* **90**, 105-111, doi:10.1016/s0304-3959(00)00392-4 (2001).
38 Tashima, R. *et al.* Optogenetic Activation of Non-Nociceptive Abeta Fibers Induces Neuropathic Pain-Like Sensory and Emotional Behaviors after Nerve Injury in Rats. *eNeuro* **5**, doi:10.1523/ENEURO.0450-17.2018 (2018).

Figure 1

A)

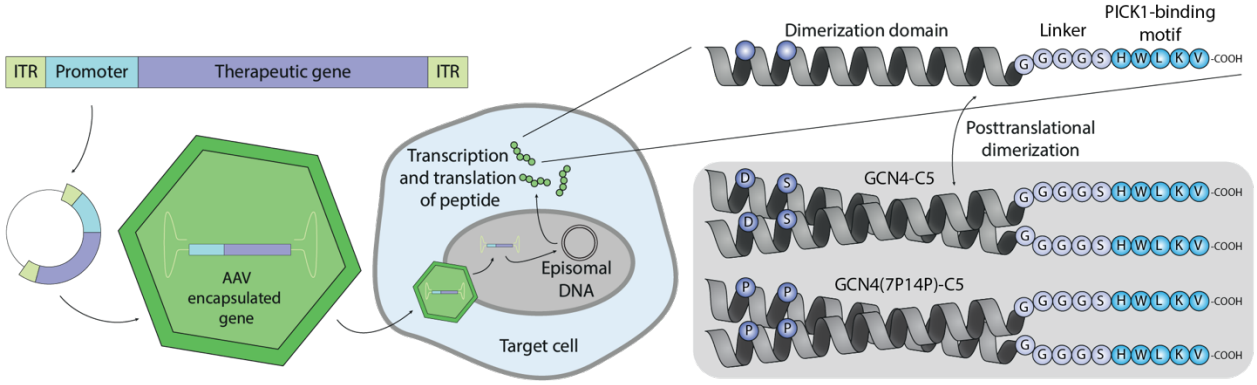

B)

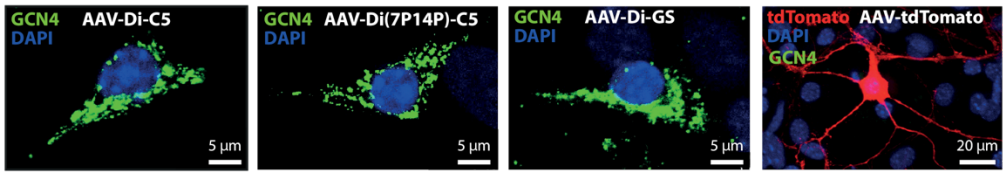

C)

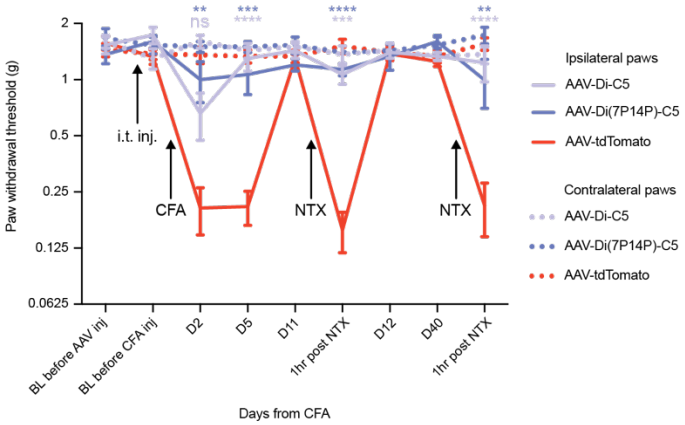

D)

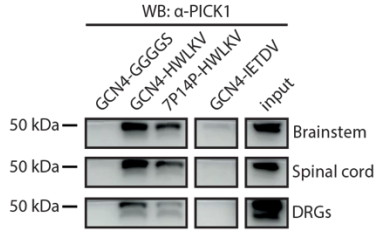

E)

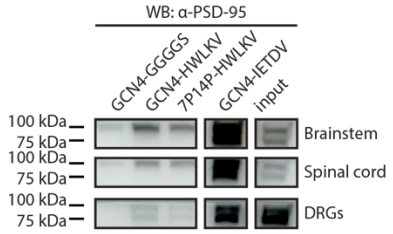

F)

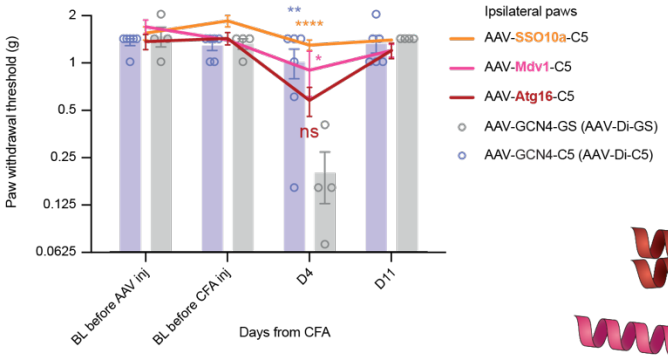

G)

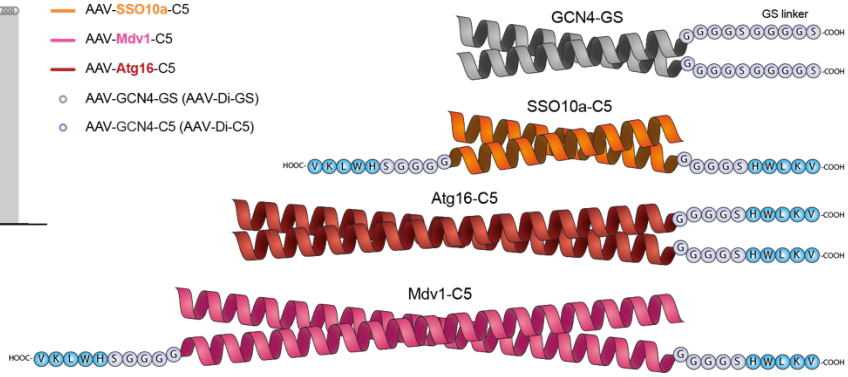

Figure 2

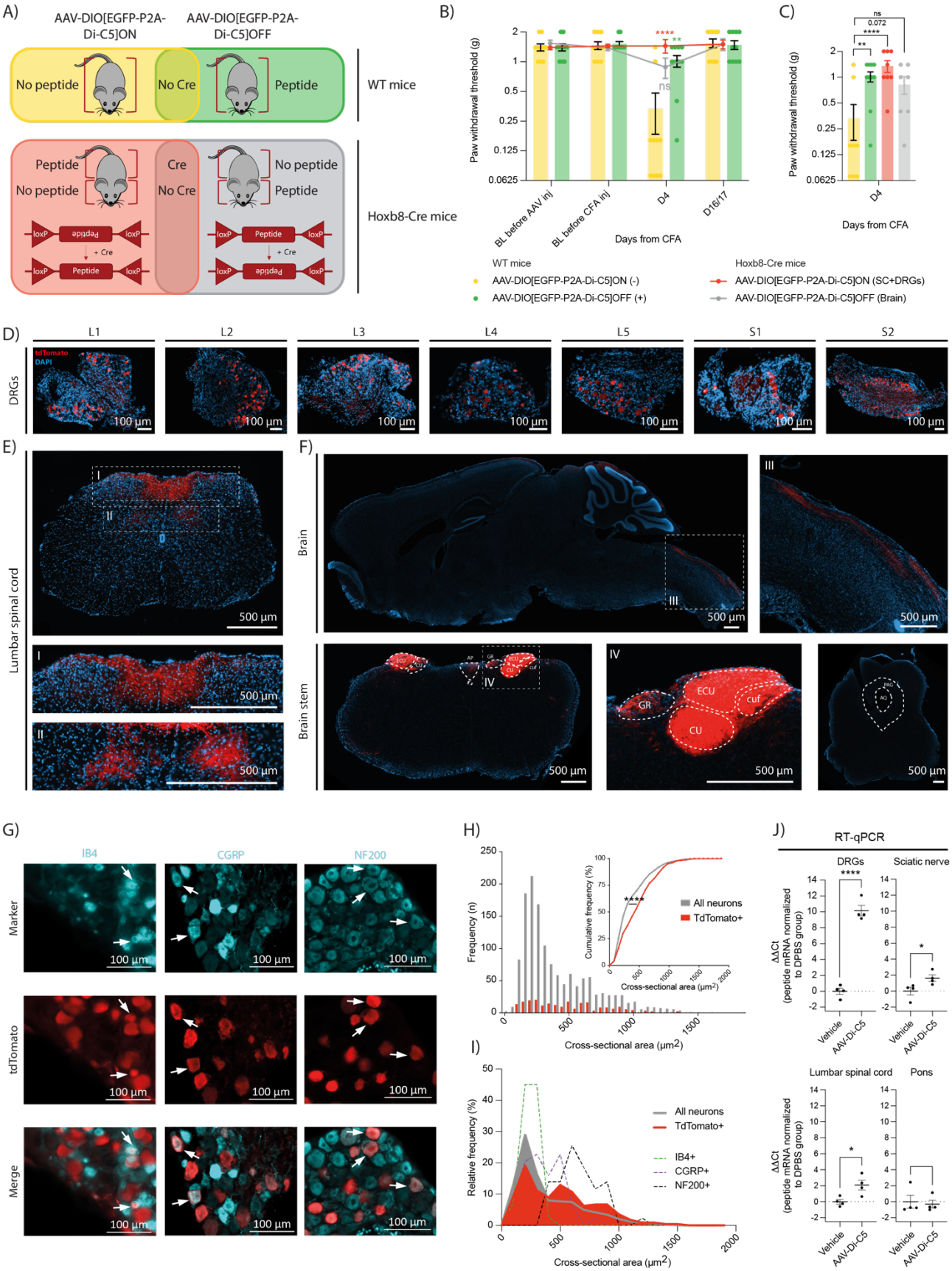
A)
AAV-DIO[EGFP-P2A-Di-C5]ON
AAV-DIO[EGFP-P2A-Di-C5]OFF
No peptide
No Cre
Peptide
WT mice
Peptide
No peptide
Cre
No Cre
No peptide
Peptide
Hoxb8-Cre mice
loxP
Peptide
+ Cre
B)
Paw withdrawal threshold (g)
BL before AAV inj
BL before CFA inj
D4
D16/17
Days from CFA
WT mice
AAV-DIO[EGFP-P2A-Di-C5]ON (-)
AAV-DIO[EGFP-P2A-Di-C5]OFF (+)
Hoxb8-Cre mice
AAV-DIO[EGFP-P2A-Di-C5]ON (SC+DRGs)
AAV-DIO[EGFP-P2A-Di-C5]OFF (Brain)
C)
Paw withdrawal threshold (g)
D4
Days from CFA
D)
L1
L2
L3
L4
L5
S1
S2
DRGs
tdTomato
DAPI
100 µm
E)
Lumbar spinal cord
500 µm
F)
Brain
Brain stem
GR
ECU
cuf
CU
500 µm
G)
IB4
CGRP
NF200
Marker
tdTomato
Merge
100 µm
H)
Frequency (n)
Cumulative frequency (%)
Cross-sectional area (µm2)
All neurons
TdTomato+
I)
Relative frequency (%)
IB4+
CGRP+
NF200+
J)
RT-qPCR
DRGs
Sciatic nerve
Lumbar spinal cord
Pons
ΔΔCt (peptide mRNA normalized to DPBS group)
Vehicle
AAV-Di-C5

Figure 3

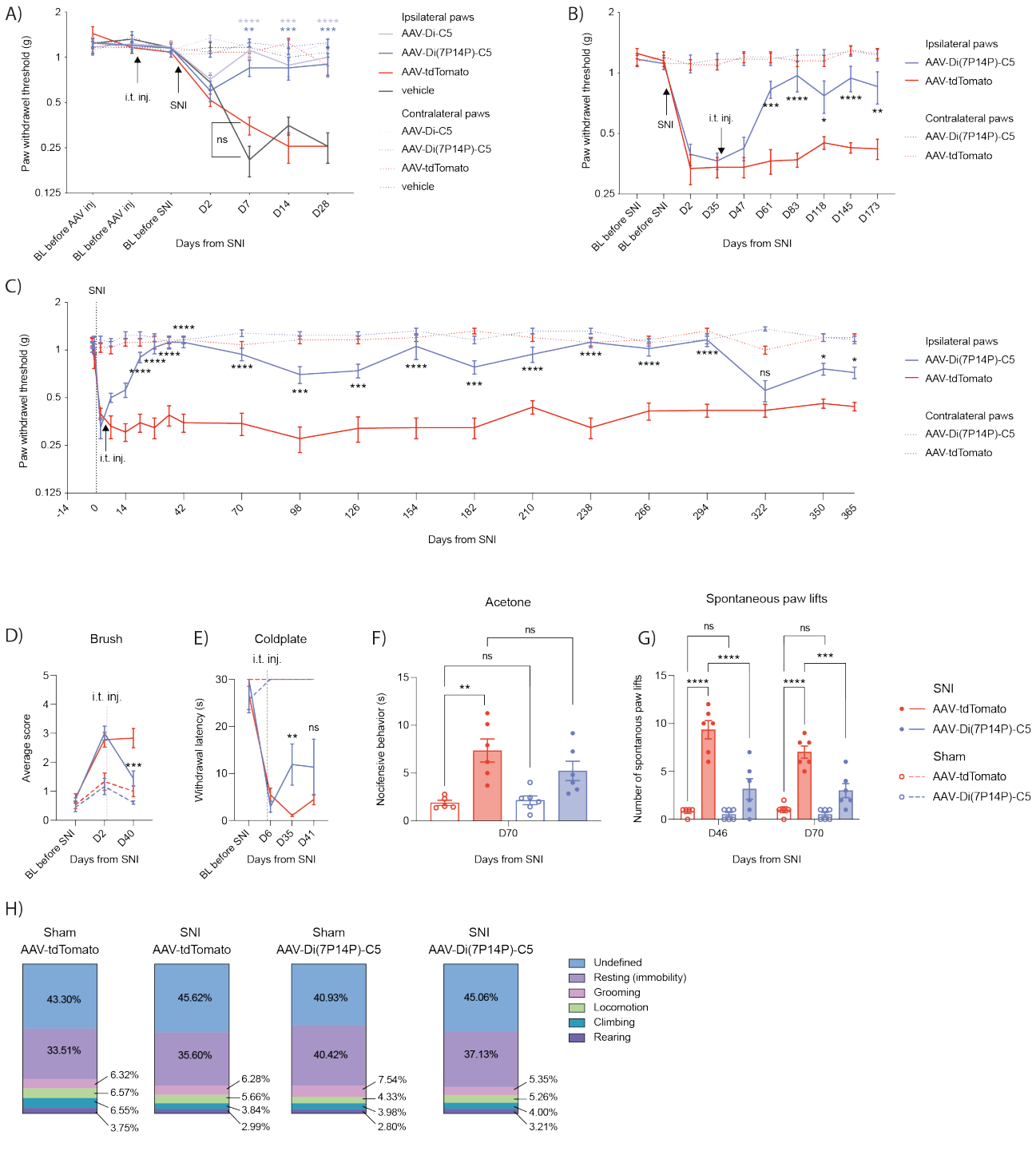
A)
Paw withdrawel threshold (g)
i.t. inj.
SNI
ns
BL before AAV inj
BL before AAV inj
BL before SNI
D2
D7
D14
D28
Days from SNI
Ipsilateral paws
AAV-Di-C5
AAV-Di(7P14P)-C5
AAV-tdTomato
vehicle
Contralateral paws
AAV-Di-C5
AAV-Di(7P14P)-C5
AAV-tdTomato
vehicle
B)
Paw withdrawel threshold (g)
SNI
i.t. inj.
BL before SNI
BL before SNI
D2
D35
D47
D61
D83
D118
D145
D173
Days from SNI
Ipsilateral paws
AAV-Di(7P14P)-C5
AAV-tdTomato
Contralateral paws
AAV-Di(7P14P)-C5
AAV-tdTomato
C)
SNI
Paw withdrawel threshold (g)
i.t. inj.
-14
0
14
42
70
98
126
154
182
210
238
266
294
322
350
365
Days from SNI
Ipsilateral paws
AAV-Di(7P14P)-C5
AAV-tdTomato
Contralateral paws
AAV-Di(7P14P)-C5
AAV-tdTomato
D)
Brush
Average score
i.t. inj.
BL before SNI
D2
D40
Days from SNI
E)
Coldplate
i.t. inj.
Withdrawal latency (s)
BL before SNI
D6
D35
D41
Days from SNI
F)
Acetone
Nocifensive behavior (s)
D70
Days from SNI
G)
Spontaneous paw lifts
Number of spontanous paw lifts
D46
D70
Days from SNI
SNI
AAV-tdTomato
AAV-Di(7P14P)-C5
Sham
AAV-tdTomato
AAV-Di(7P14P)-C5
H)
Sham AAV-tdTomato
SNI AAV-tdTomato
Sham AAV-Di(7P14P)-C5
SNI AAV-Di(7P14P)-C5
43.30%
33.51%
6.32%
6.57%
6.55%
3.75%
45.62%
35.60%
6.28%
5.66%
3.84%
2.99%
40.93%
40.42%
7.54%
4.33%
3.98%
2.80%
45.06%
37.13%
5.35%
5.26%
4.00%
3.21%
Undefined
Resting (immobility)
Grooming
Locomotion
Climbing
Rearing

Figure 4

A)

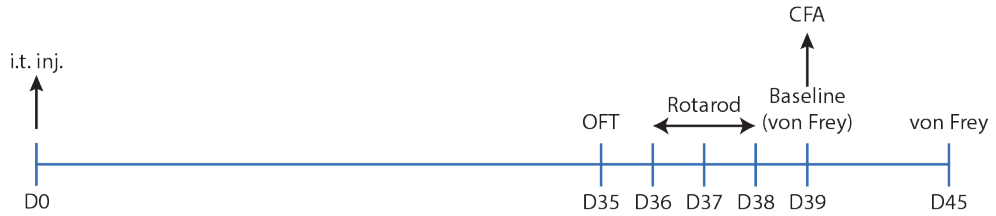

Open Field Test

B)

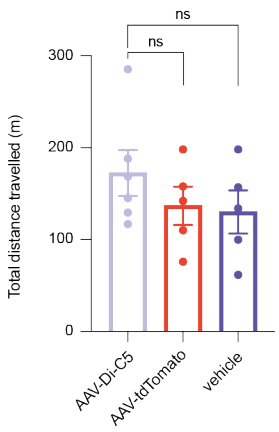

C)

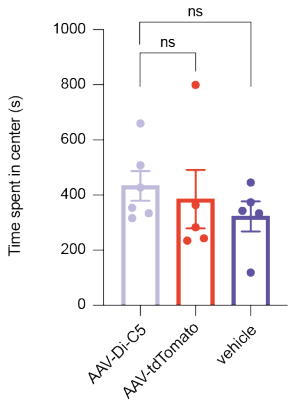

D)

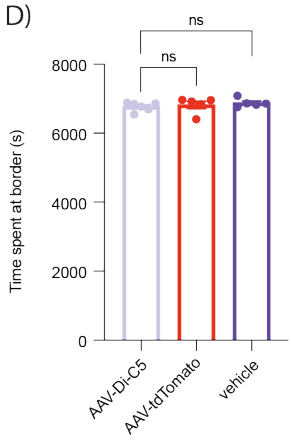

RotaRod

E)

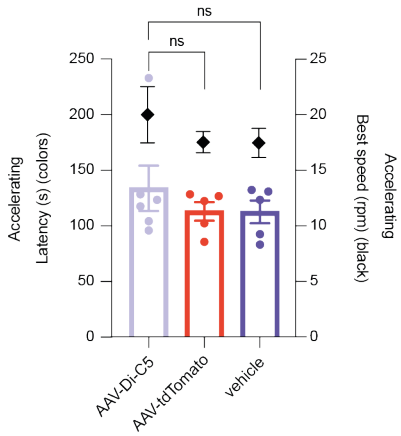

F)

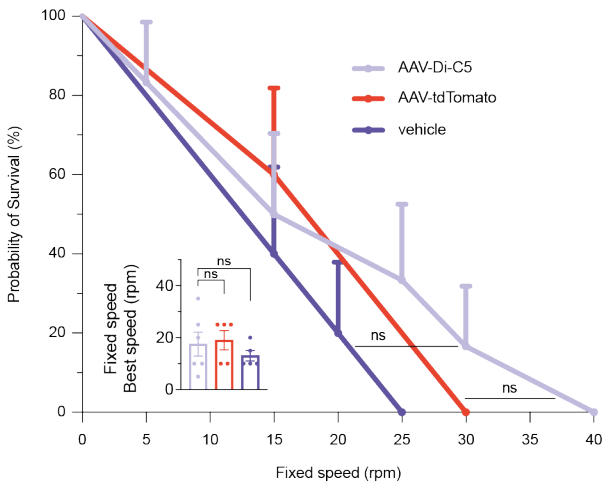

Figure 5

A)

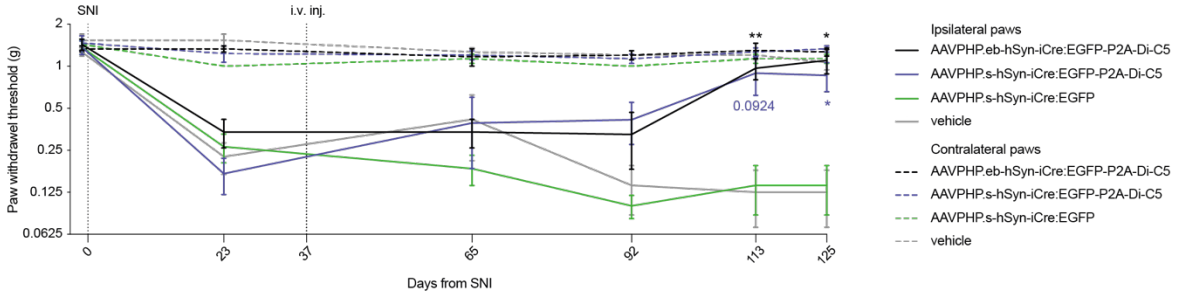
SNI
i.v. inj.
Paw withdrawel threshold (g)
2
1
0.5
0.25
0.125
0.0625
0
23
37
65
92
113
125
Days from SNI
**
*
0.0924
*
Ipsilateral paws
AAVPHP.eb-hSyn-iCre:EGFP-P2A-Di-C5
AAVPHP.s-hSyn-iCre:EGFP-P2A-Di-C5
AAVPHP.s-hSyn-iCre:EGFP
vehicle
Contralateral paws
AAVPHP.eb-hSyn-iCre:EGFP-P2A-Di-C5
AAVPHP.s-hSyn-iCre:EGFP-P2A-Di-C5
AAVPHP.s-hSyn-iCre:EGFP
vehicle

B)

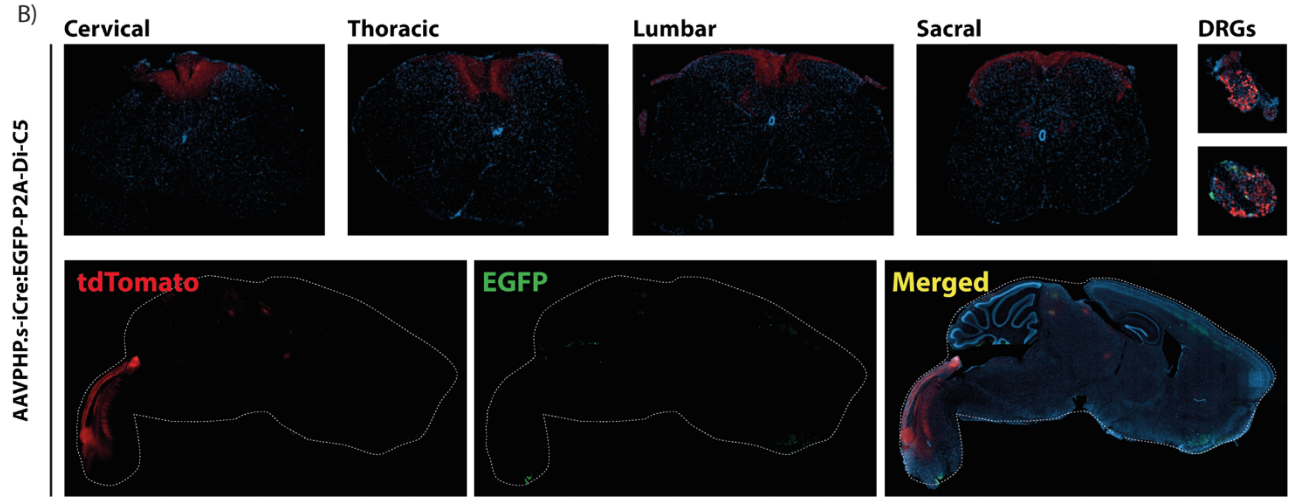
Cervical
Thoracic
Lumbar
Sacral
DRGs
AAVPHP.s-iCre:EGFP-P2A-Di-C5
tdTomato
EGFP
Merged

C)

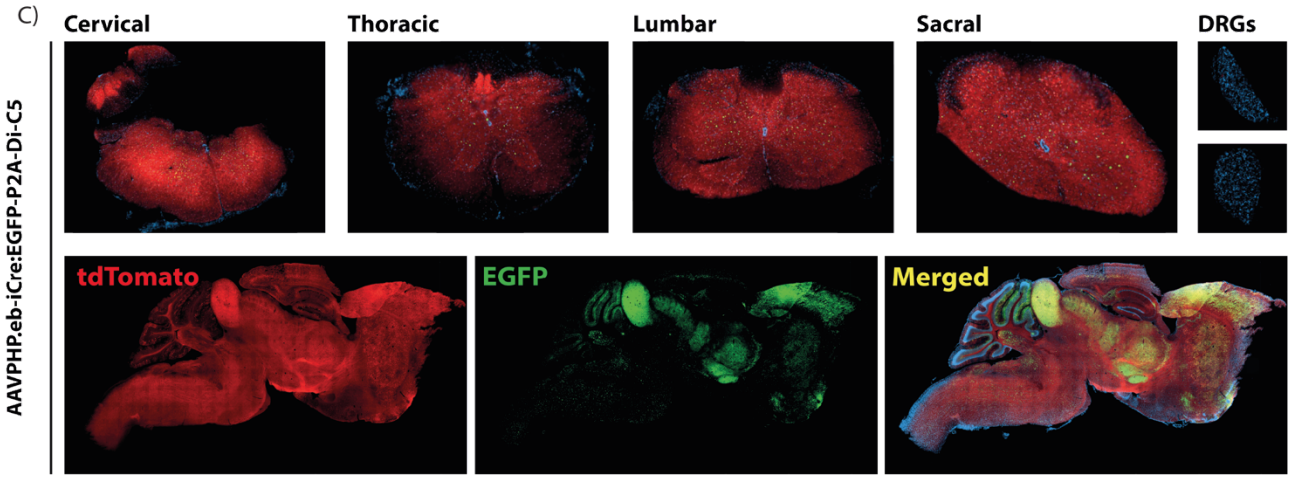
Cervical
Thoracic
Lumbar
Sacral
DRGs
AAVPHP.eb-iCre:EGFP-P2A-Di-C5
tdTomato
EGFP
Merged